

Laser peeler regime of high-harmonic generation for diagnostics of high-power focused laser pulses

Cite as: Matter Radiat. Extremes 8, 034402 (2023); doi: 10.1063/5.0142051

Submitted: 11 January 2023 • Accepted: 15 March 2023 •

Published Online: 3 April 2023





View Online



Export Citation



CrossMark

S. E. Perevalov,^{1,a)}  A. M. Pukhov,²  M. V. Starodubtsev,¹  and A. A. Soloviev¹ 

AFFILIATIONS

¹Institute of Applied Physics of the Russian Academy of Sciences, 46 Ulyanov st., Nizhny Novgorod 603950, Russia

²Institut für Theoretische Physik I Heinrich-Heine-Universität Düsseldorf, Universitätsstraße 1, 40225 Düsseldorf, Germany

^{a)}Author to whom correspondence should be addressed: perevalov@ipfran.ru

ABSTRACT

A method for measuring the intensity of focused high-power laser pulses based on numerical simulation of high-harmonic generation in the laser peeler regime is proposed. The dependence of the efficiency of high-harmonic generation on the laser pulse intensity and the spatial parameters during interaction with solid targets is studied numerically. The simulation clearly shows that the amplitude of the generated harmonics depends on the laser pulse parameters. The proposed method is simpler than similar intensity measurement techniques and does not require complex preparation.

© 2023 Author(s). All article content, except where otherwise noted, is licensed under a Creative Commons Attribution (CC BY) license (<http://creativecommons.org/licenses/by/4.0/>). <https://doi.org/10.1063/5.0142051>

I. INTRODUCTION

Measuring the peak intensity of focused laser pulses of sub-petawatt and petawatt power is an important current challenge. Standard (semiconductor) detectors are not fit for this, since they can be used only for pulses with intensities no higher than 10^{11} W cm⁻². If a laser pulse is attenuated on Fresnel reflection from an uncoated glass surface, phase and/or spectral distortions may emerge in the resulting pulse. There are various methods for direct intensity measurements based on the interaction of intense laser pulses with a low-density plasma. One of these is peak laser intensity measurement via scattering of electrons or protons in a laser focal spot.¹ This method requires a regime of laser-plasma interaction in which Coulomb interactions between the particles can be neglected. This imposes certain conditions on the ambient vacuum, as well as some restrictions on the parameters of the gas or solid target used to measure the intensity. In addition, the diagnostics used in these experiments must be highly sensitive to a small number of particles participating in the laser-plasma interaction. Another method for direct measurement of peak laser intensity is based on the observation of multiple sequential tunneling ionization of atoms and the study of the spectra of multiply charged ions² formed in the field of high-intensity laser pulses. This method also requires exotic conditions for the targets and complicated time-of-flight

spectrometers highly sensitive to a small number of particles. In addition, this method has a threshold effect.

In this work, we propose to use the high-harmonic generation (HHG) that occurs during the interaction of laser pulses with solid targets as a direct method for measuring peak laser intensity. It is well known that high harmonics can be generated in the coherent wake emission (CWE) regime³ at intensities up to 10^{18} W cm⁻² or, for example, in the relativistic oscillating mirror (ROM) regime⁴ at higher intensities of the order of 10^{21} W cm⁻². In these regimes, laser pulses are incident at a large angle to the target surface. In this case, the efficiency of generation of high harmonics and their maximum number depend on the laser pulse intensity, and thus these regimes can be used for direct intensity measurements. Besides, complex diagnostics or exotic experimental conditions are not needed for measuring high-harmonic spectra. However, the resulting spectra of high harmonics in these two regimes decrease rapidly with increasing harmonic number, which can substantially reduce measurement accuracy. It was recently shown that when a laser pulse is incident on a target along its surface, the spectra of high harmonics are flatter, close to n^{-1} ,⁵ owing to an increase in the interaction length. This advantage can improve the accuracy of laser radiation intensity measurements. Such a regime is called a “laser peeler.”⁶ In the present paper, we propose to diagnose peak laser intensity based on this regime of HHG. From the experimental point of view, it

is more convenient to use a laser pulse incident at a small angle rather than along the target as in Ref. 6. This approach simplifies target alignment in experiments. The spectra of high harmonics, which change with changes in the intensity, are measured experimentally. To determine the intensity, the experimental results should be correlated with calculations performed using particle-in-cell simulations. Since the spectra of high harmonics simulated in different modes (1D and 2D) are in good agreement with the experimental data,^{3,7,8} it is convenient to use this method for calculating the intensity dependence of the spectra of high harmonics. It is clear that at constant focusing parameters, the intensity of a focused laser pulse depends on the duration and energy of the pulse. The duration cannot be unambiguously measured in experiments, since these measurements are made using attenuation either by averaging over the beam aperture or locally at the “hot” point of the aperture. At the same time, the pulse energy can be determined with much higher accuracy. Therefore, to obtain the dependence of high-harmonic spectra on laser pulse parameters in a simulation, it is necessary to fix the energy and change the peak intensity by varying the duration. Thus, by correlating the experimentally measured spectra and those obtained from the simulation, it is possible to determine with high accuracy the intensity at the focal point when the pulse is focused on the target.

II. METHODS

The numerical study was performed using a particle-in-cell simulation with the Virtual Laser Plasma Lab (VLPL) code.⁹ A 2D version of the 3D VLPL code was used, in which the third dimension is reduced to a single cell. To resolve a sufficient number of harmonics, we chose a time step of $0.002\lambda_0 c^{-1}$, where c is the speed of light in vacuum. Such a step allows observation of harmonics up to number 500. The simulation area had dimensions $x \times y \times z = 20\lambda_0 \times 20\lambda_0 \times 1\lambda_0$, with steps $dx = 0.002\lambda_0$ along x and $dy = 0.02\lambda_0$ along y . This reduced distortions, including weakening the accumulation of noise during calculations, while at the same time speeding up the calculation. The calculation was made in a moving window mode with kernel partitioning $x \times y \times z = 256 \times 1 \times 1$ using the resources of the Joint SuperComputer Center of the Russian Academy of Sciences (JSCC RAS). At each simulation step, the field was recorded at the left (incident radiation) and right (reflected, generated radiation) boundaries. In this way, spatiotemporal distributions of the fields were formed at the window boundaries, enabling their Fourier analysis and determining frequency-spatial spectra. In these spectra, the frequencies are normalized to the central (fundamental) frequency ω_0 with dimensionless amplitude A_0 , and the projections k_y of the wave vector on the y axis are normalized to the modulus k of the wave vector for the central wavelength corresponding to λ_0 . In the course of spectral reconstruction, the time grid was transformed to a frequency grid, as is typical for the Fourier transform:

$$f = \frac{[0, \dots, \frac{1}{2}(N_t - 1)]}{N_t dt},$$

where f is the frequency, N_t is the time grid number of points, and dt is the time grid step. Analogously, the y coordinate was converted to spatial y frequencies.

$$f_y = \frac{[0, \dots, \frac{1}{2}(N_y - 1)]}{N_y dy},$$

where N_y is the number of grid points along the y coordinate and dy is the grid step along y . Frequency normalization to the fundamental frequency allows us to pass to the harmonic number $n = 2\pi f/\omega_0$. The spatial y frequency is normalized analogously, with the normalized wave number being $k_y/k_0 = 2\pi f_y c/\omega_0$.

III. RESULTS

The laser pulse in the simulation was focused with an angle of $f/4$. The minimal angle of incidence of the laser pulse in this case was $\phi = 6.34^\circ$ ($k_x/k_0 = 0.9$, $k_y/k_0 = -0.1$), which corresponds to half the focusing angle $f/4$ (Fig. 1). The laser pulse had a Gaussian spatial distribution and time envelope $\cos^2 t$.

The laser pulse energy was fixed at a level of 5.6 J, which for $4 \mu\text{m}$ (FWHM) and a duration of 30 fs (FWHM) corresponds to a dimensionless amplitude $a_0 = 30$, where $a_0 = \sqrt{7.3 \times 10^{-19} \lambda^2 [\mu\text{m}] I_0 [\text{W cm}^{-2}]}$. Later, only a_0 changed with a variation of duration, and the pulse was not chirped. The central wavelength of 910 nm corresponds to the central wavelength of the laser complex PEARL.¹⁰ The target consisted of hydrogen, which corresponds to the plastic target in the experiment. The density was fixed at $N_e = 30N_{cr}$, where $N_{cr} = 11.134 \times 10^{20}/\lambda^2 (\mu\text{m})$ is the critical density for the central wavelength λ_0 . When a laser pulse interacts with a target, a surface plasma wave is excited on it, the wave period of which coincides with the period of the incident field [Fig. 2(a)].

Plasma tongues aligning across the target and moving along the laser pulse coincide in time with half-waves, when the field is positive, i.e., directed from the target. The reflected field [Figs. 2(b) and 3] is strongly distorted; the duration of individual peaks amounts to several hundred attoseconds, with characteristic sharp peaks only in the negative half-waves of the reflected field. The corresponding spectra [Fig. 3(a)] feature a large number of high harmonics. The spatial distributions [Fig. 2(c)] demonstrate that high harmonics are generated at an angle corresponding to the angle of

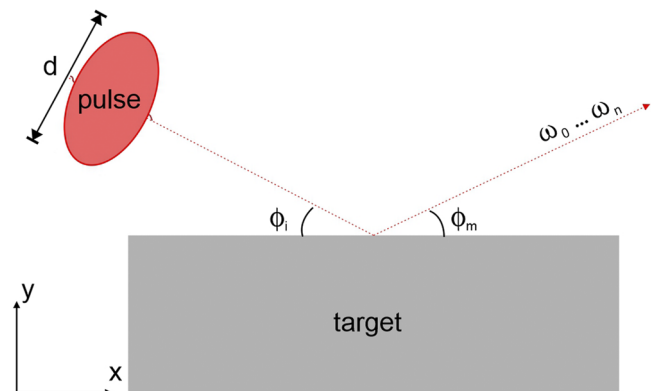


FIG. 1. Scheme of numerical simulation of HHG. d is the transverse dimension at full width at half maximum (FWHM), ϕ_i is the angle of incidence, ϕ_m is the angle of reflection, and $\omega_0, \dots, \omega_n$ are generated harmonics.

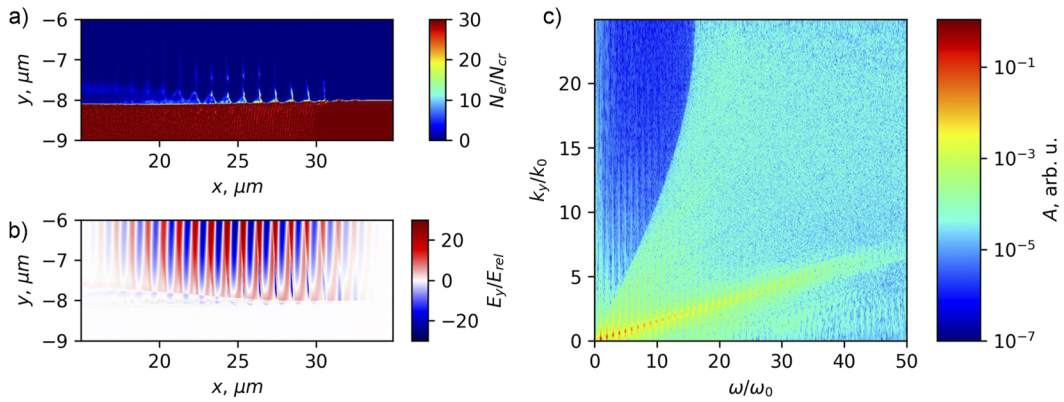


FIG. 2. (a) Typical electron density distribution in units of N_{cr} , (b) field component E_y in units of the relativistic electric field E_{rel} , and (c) spatial spectrum of high harmonics in arbitrary units for 30 fs, focusing $f/4$, and $a_0 = 30$.

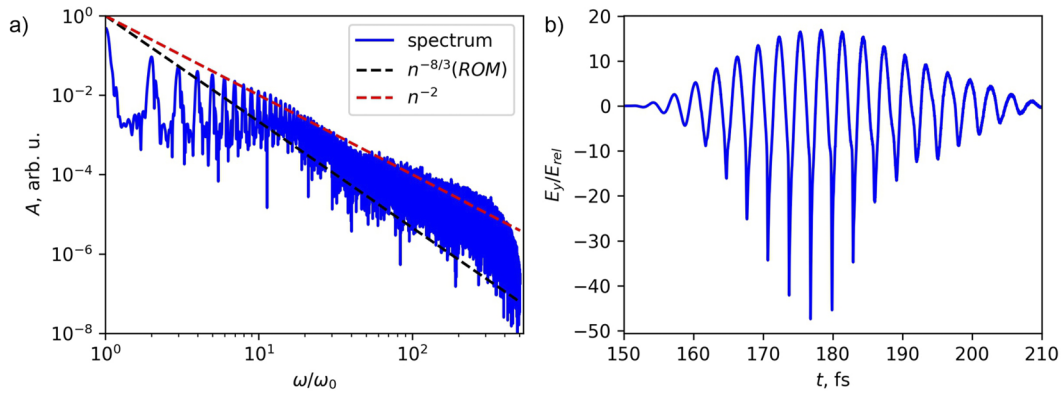


FIG. 3. (a) Typical spectrum of generated high harmonics in arbitrary units for the parameters of Fig. 2 and (b) typical time profile of electric field component after the interaction of the laser pulse with the target surface in units of E_{rel} for 30 fs, focusing $f/4$, and $a_0 = 30$.

incidence of the laser pulse on the target. It can also be seen that all harmonics are generated at the same angle.

IV. DISCUSSION

A. Correlation between high-harmonic spectra and incident pulse intensity

Changes in the peak intensity with variations in the duration and in the fixed energy of the laser pulse incident on the target lead to a decrease or an increase in the HHG efficiency, which is seen in the integrated spectra (Fig. 4). These were obtained by integrating the spatial spectra [Fig. 2(c)] in the $\pm 6^\circ$ range of reflection angle. The range of angles was chosen based on the fact that the angle of reflection is approximately equal to 6° and the field generated at an angle less than 0° to the target does not reach the “detector,” which must be located in mirror order relative to the incident pulse. The integral spectra for three laser pulses of different duration and, accordingly, a_0 , are shown in Fig. 4, since these three series have the same energy. Note that not only does the amplitude of the harmonics change, increasing in cases of higher intensity, but so too does their maximum number (cutoff). On the whole, similarly to the case of laser

pulse incidence along the target, the spectra are flatter than in other regimes of HHG.^{3,4}

From the graphs for the amplitude of the harmonic with number n , one can see that with a decrease in the laser pulse intensity, the amplitudes of all harmonics decrease [Figs. 5(a) and 5(c)]. Since the interaction process is complex and its dynamics are nonlinear, the normalized amplitudes of all harmonics at a fixed intensity do not coincide. The general form of the dependence can be obtained by considering a certain value averaged over all harmonics or a set of harmonics:

$$A(I_l) = \frac{A_1(I_l)}{\max[A_1(I_l)]} + \frac{A_2(I_l)}{\max[A_2(I_l)]} + \dots + \frac{A_n(I_l)}{\max[A_n(I_l)]},$$

where I_l is the laser pulse intensity and A_n is the n th-harmonic amplitude normalized to the amplitude of the fundamental harmonic (A_0). The resulting curve qualitatively describes the behavior of any harmonic with $n > 1$, where only the proportionality factor depends on the number. The curves obtained from the simulation are shown in Figs. 5(b) and 5(d).

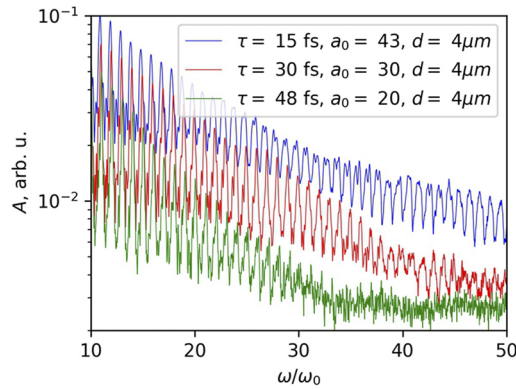


FIG. 4. Integral spectra of high harmonics at different laser pulse intensities. The colors show the spectra for different laser pulse intensities. The amplitude is in arbitrary units.

For experimental determination of laser pulse intensity or duration at fixed energy, it is necessary to measure the amplitude of some selected or all visible harmonics. The set can contain any convenient number of harmonics. Since the detector in our experiments measures energy rather than amplitude, i.e., there is integration over time, it is necessary to take the harmonic signal measured by

the detector to the power of $1/2$, thereby obtaining the integral of the field modulus. Any harmonic can be used as normalization, for example, a harmonic with the smallest recorded number. The values obtained should be compared with the corresponding simulated dependences, with normalization for the harmonic with a respective number. A straight line perpendicular to the x axis and passing through the points will show the peak intensity at the target. However, as can be seen from a comparison of Figs. 5(a) and 5(c) and Figs. 5(b) and 5(d), the number of the high harmonic starting from which intensity may be measured should be chosen very carefully. Higher harmonics grow faster with increasing intensity, with a power law close to n^{-1} , than lower harmonics. Thus, by choosing only high harmonics, one can significantly reduce the measurement error of peak intensity. In addition, the efficiency of generating high harmonics depends on the depth of focusing on the target (see Sec. IV B).

B. Impact of focusing parameters

With small changes in the angle of incidence, the spectra of the generated harmonics are in a good agreement to experimental accuracy (Fig. 6), which is very convenient for experiment. This somewhat weakens the requirements for targeting, and it can be asserted that a 1° miss in angle will not affect the experimental result.

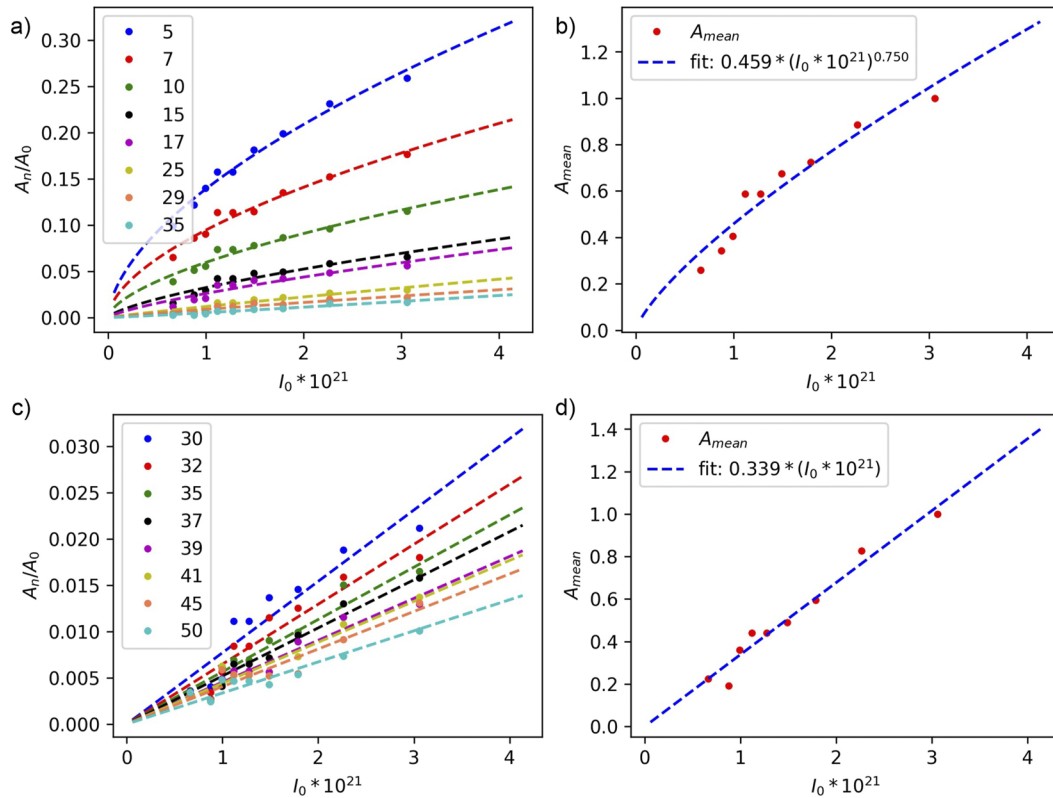


FIG. 5. Relative amplitude of harmonics [(a) and (c)] and averaged relative amplitude [(b) and (d)] as functions of incident laser pulse intensity (in W/cm^2); different harmonics are shown by different colors. Dashed lines show approximation by a power function in (a) and (b) and approximation by a linear function in (c) and (d).

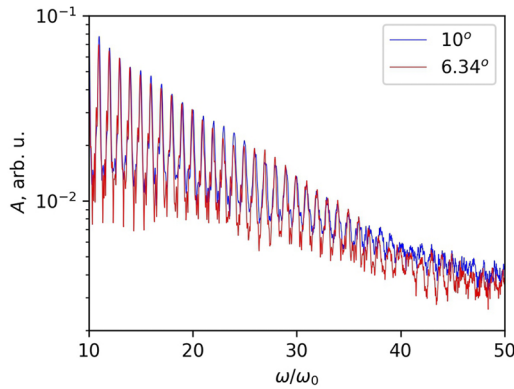


FIG. 6. Comparison of the integrated spectra of HHG at different angles of incidence of the laser pulse on the target for 30 fs, focusing $f/4$, and $a_0 = 30$. Spectra at different angles of incidence are shown by color. The amplitude is in arbitrary units.

According to Ref. 7, there should be a decrease in high-harmonic output when the angle of incidence decreases from 10° to 6.34° by about 50%; however, this is not observed, as can be seen from Fig. 6. This can be explained by the inapplicability of the model from

Ref. 7 for the interaction mode considered in this paper, since this model does not take into account the increase in the interaction length with a decrease in the angle of incidence. In addition, the accuracy of pointing laser pulses to a flat target significantly exceeds 1° .

Figure 7 shows the results of simulation the generation of high harmonics at different focusing depths D (i.e., at different positions of the focal waist with respect to the target within two Rayleigh lengths). It can be seen that the amplitudes of low harmonics [Fig. 7(a)] and their averaged value [Fig. 7(b)] increase when the laser beam waist is located in front of the target. This means that low harmonics (lower than $n \sim 30$) should not be used for measuring the peak intensity of laser radiation, since inaccurate targeting can lead to erroneous interpretation of measurement results and a significantly overestimated value of the intensity. However, when considering a separate contribution of high harmonics [Fig. 7(c)], it can be seen that they experience a much smaller change, when the focus shifts within the studied limits. Thus, for the considered laser pulse parameters, high harmonics with numbers higher than 35 should be used for measuring intensity. At the same time, it should be noted that averaging over harmonics, for example, 30, 32, 35, 37, 39, 41, and 45 [Fig. 7(d)], gives a measurement error of no more than 15%, with an error in the focusing depth of up to $60 \mu\text{m}$.

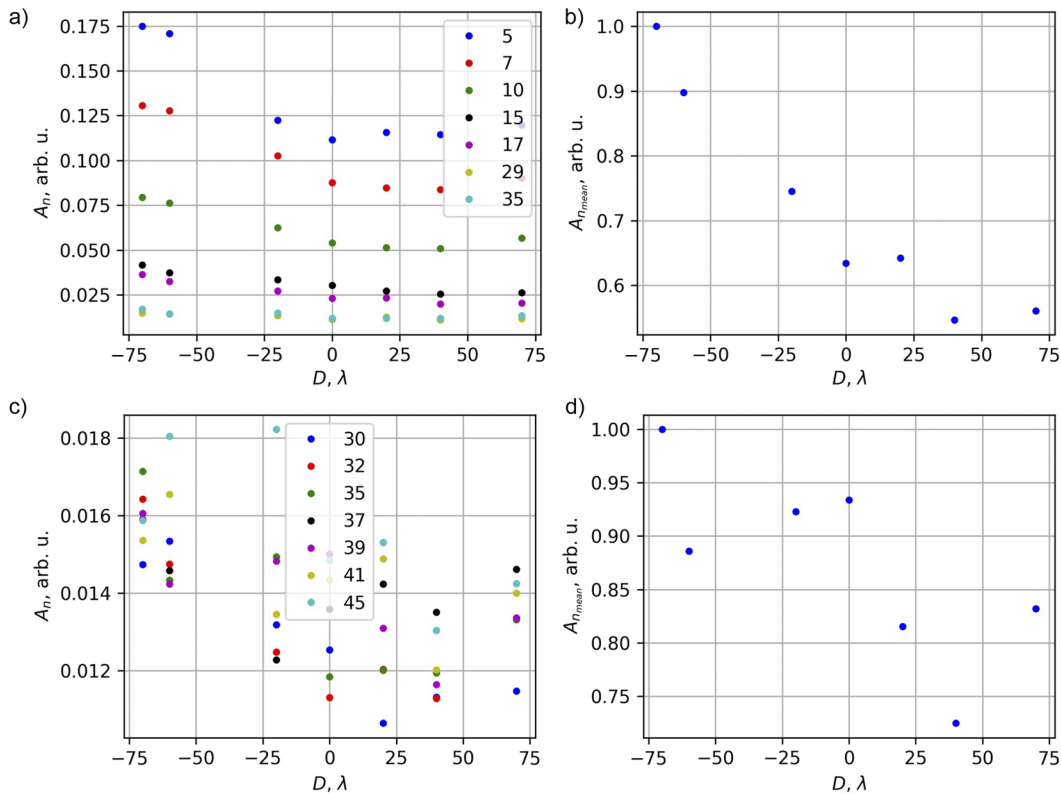


FIG. 7. (a) and (c) Amplitudes of low (a) and high (c) harmonics as functions of focusing depth D for 30 fs, focusing $f/4$, and $a_0 = 30$; the amplitudes of different harmonics are shown by different colors. (b) and (d) Averaged relative amplitudes of harmonics as functions of focusing depth, taking into account low harmonics (b) and only high harmonics (d).

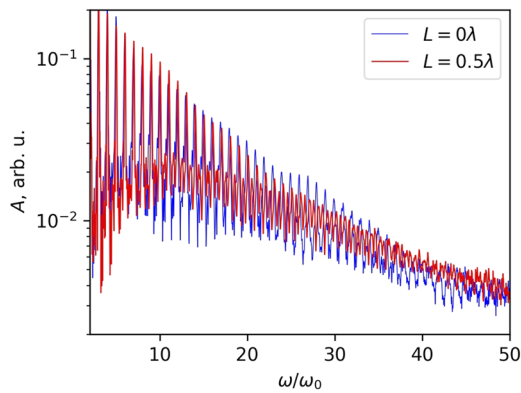


FIG. 8. Comparison of integrated spectra with and without density gradient for 30 fs, focusing $f/4$, and $a_0 = 30$. Spectra are shown in color for different density gradients. The amplitude is in arbitrary units.

Taking into account the fact that the Rayleigh length is about $28 \mu\text{m}$, which determines the accuracy of focusing on the target, the error is even smaller. When considering individual harmonics, for example 35, the error at $60 \mu\text{m}$ is about 30%.

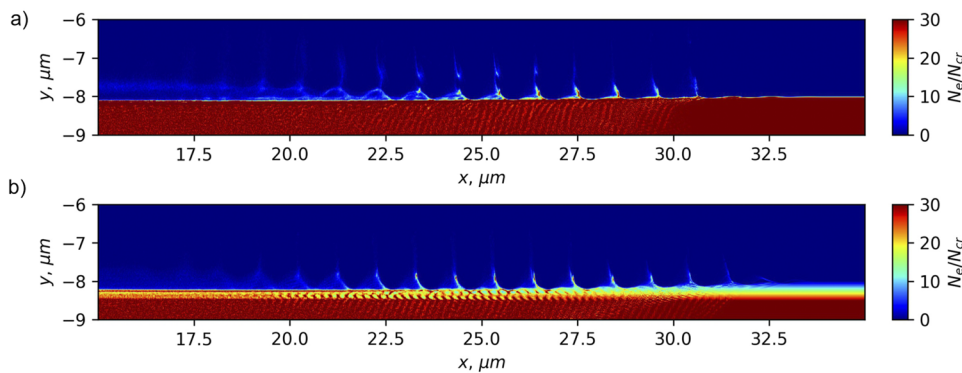


FIG. 9. Density distribution at the moment of interaction of the laser pulse center with the target in the case of a sharp boundary (a) and in the case of a linear growth with $L = 0.5\lambda_0$ (b) for 30 fs, focusing $f/4$, and $a_0 = 30$. The density is normalized to N_{cr} .

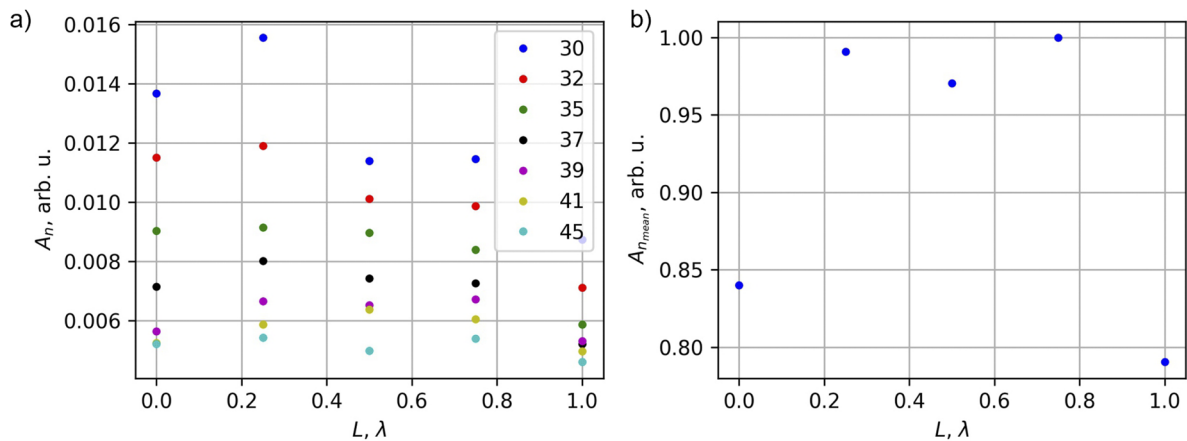


FIG. 10. (a) Amplitude of high harmonics as a function of density gradient scale for 30 fs, focusing $f/4$, and $a_0 = 30$; the amplitudes of different harmonics are shown by different colors. (b) Averaged relative amplitude of harmonics as a function of density gradient scale.

C. Impact of laser pulse contrast on harmonic generation

A nano- or subnanosecond contrast of the order of 10^9 in laser pulses, which is typical for many laser systems, including optical parametric chirped pulse amplification (OPCPA) ones, inevitably leads to the emergence of a preplasma when such laser pulses are focused on the target surface. The preplasma forms a density gradient, frequently resulting in differences between experimental results and theory. The scale of the gradient depends on the prepulse intensity on the target and usually corresponds to plasma expansion with ion-acoustic speed. The mechanisms of HHG, namely, CWE and ROM, have been reviewed in Ref. 7. For the conditions of our study, the ROM mechanism is most suitable, since it is implemented at intensities similar to ours. With a variation in the scale of the plasma density gradient on the target surface from $\lambda/20$ to $\lambda/5$, the generation of high harmonics in the high-frequency region increases and the spectrum approaches $n^{-8/3}$,¹¹ which has been observed in other experiments as well.^{12,13} Enhancement of generation on reflection from relativistic plasma mirrors with a gradient of the order of c/λ_0 is associated with the appearance of resonance.⁸ At the same time, with a decrease in the angle of incidence, an optimum is observed at angles of about 30° (for $\lambda/20$), and so it is expected that the presence of a gradient of the order of 100–500 nm, together with a small

angle of incidence, will not affect HHG in the ROM regime, assuming the effects are equal. For observing the evolution of HHG with a plasma density gradient on the surface under our conditions, we will simulate such a situation. At $a_0 = 30$ and a duration of 30 fs, for a density of $N_e = 30N_{cr}$, the density gradient will be set for simplicity in the form of a linear growth with length $L = 0.5\lambda_0$, which usually corresponds to a nano- to subnanosecond prepulse with an intensity of the order of $10^{12} \text{ W cm}^{-2}$ (1 mJ per 1 ns).^{14,15} In the papers cited above, a gradient in which the plasma density profile is represented as a decreasing decaying exponential function is considered. Since the gradient is actually somewhat larger, the linear approximation will be closer to reality.

Figures 2–7 show the simulation results without the density gradient on the target surface. As can be seen from Fig. 8, the presence of a linear growth of plasma density (Fig. 9) with a length of $0.5\lambda_0$ has little effect on the harmonics output. This effect is probably not related to the studied geometry. Most likely, the weak effect of the density gradient is related to the dynamics of the surface plasma wave, which requires a separate study. The greatest difference in the region of harmonics from 30 to 50 is less than 5%. Such a difference will inevitably introduce an error in peak intensity measurements.

This can also be seen from Fig. 10, which shows the amplitudes of high harmonics as a function of the density gradient on the target surface. In total, for the harmonics in the region of 20–50, the relative error that the technique gives can be about 35%. Consideration of high harmonics with averaging in the range from 40 and above will lead to a significant reduction in the error, at least due to the effect depicted in Fig. 7. Although the simulation results are given for intensities around $10^{21} \text{ W cm}^{-2}$, the measurement method is suitable for higher intensities of up to $10^{23} \text{ W cm}^{-2}$. However, it may be necessary to select the target material to minimize the effect of ion motion, which occurs in the case of high intensities, for which additional research is planned.

V. CONCLUSION

Measurement of the peak intensity of focused high-power laser pulses is currently a highly relevant problem. However, today there are few methods for its direct measurement, and all of them impose certain requirements on the organization of the experiment, both on the accuracy of the achieved parameters and on the complexity of the diagnostic methods used. Using the approach proposed here makes it possible to greatly simplify the experiment, at least by simplifying the diagnostics. The proposed method of intensity measurements is based on high-harmonic generation in the laser peeler regime. Numerical simulation has shown that this technique can be successfully used in experiments with fairly simple requirements on targeting and on the experimental conditions. The method can be implemented over a wide range of focusing angles and is insensitive to nano- and subnanosecond prepulses. This and its fairly simple diagnostics are undoubted advantages of the proposed technique.

ACKNOWLEDGMENTS

This work was supported by the Russian Science Foundation within the framework of Project No. 20-62-46050. The authors

would like to thank the Joint SuperComputer Center of the Russian Academy of Sciences for access to computing resources.

AUTHOR DECLARATIONS

Conflict of Interest

The authors have no conflicts to disclose.

Author Contributions

S. E. Perevalov: Conceptualization (equal); Data curation (equal); Formal analysis (equal); Investigation (equal); Visualization (equal); Writing – original draft (equal); Writing – review & editing (equal). **A. M. Pukhov:** Investigation (equal); Methodology (equal); Software (equal). **M. V. Starodubtsev:** Conceptualization (equal); Formal analysis (equal); Investigation (equal); Writing – review & editing (equal). **A. A. Soloviev:** Funding acquisition (equal); Project administration (equal); Writing – review & editing (equal).

DATA AVAILABILITY

The data that support the findings of this study are available from the corresponding author upon reasonable request.

REFERENCES

- ¹O. E. Vais and V. Yu Bychenkov, “Complementary diagnostics of high-intensity femtosecond laser pulses via vacuum acceleration of protons and electrons,” *Plasma Phys. Controlled Fusion* **63**, 014002 (2020).
- ²M. F. Ciappina and S. V. Popruzhenko, “Diagnostics of ultra-intense laser pulses using tunneling ionization,” *Laser Phys. Lett.* **17**, 025301 (2020).
- ³F. Quéré, C. Thauray, P. Monot, S. Dobosz, P. Martin, J.-P. Geindre, and P. Audebert, “Coherent wake emission of high-order harmonics from overdense plasmas,” *Phys. Rev. Lett.* **96**, 125004 (2006).
- ⁴C. Thauray, F. Quéré, J.-P. Geindre, A. Levy, T. Ceccotti, P. Monot, M. Bougeard, F. Réau, P. d’Oliveira, P. Audebert, R. Marjoribanks, and P. Martin, “Plasma mirrors for ultrahigh-intensity optics,” *Nat. Phys.* **3**, 424–429 (2007).
- ⁵X. F. Shen, A. Pukhov, and B. Qiao, “Synergistic longitudinal acceleration and transverse oscillation in high-order harmonic generation,” *arXiv:2009.12918* (2020).
- ⁶X. F. Shen, A. M. Pukhov, S. E. Perevalov, and A. A. Soloviev, “Electron acceleration in intense laser–solid interactions at parallel incidence,” *Quantum Electron.* **51**, 833 (2021).
- ⁷C. Thauray and F. Quéré, “High-order harmonic and attosecond pulse generation on plasma mirrors: Basic mechanisms,” *J. Phys. B: At., Mol. Opt. Phys.* **43**, 213001 (2010).
- ⁸U. Teubner and P. Gibbon, “High-order harmonics from laser-irradiated plasma surfaces,” *Rev. Mod. Phys.* **81**, 445 (2009).
- ⁹A. Pukhov, “Three-dimensional electromagnetic relativistic particle-in-cell code VLPL (virtual laser plasma lab),” *J. Plasma Phys.* **61**, 425 (1999).
- ¹⁰V. V. Lozhkarev, G. I. Freidman, V. N. Ginzburg, E. V. Katin, E. A. Khazanov, A. V. Kirsanov, G. A. Luchinin, A. N. Mal’shakov, M. A. Martyanov, O. V. Palashov, A. K. Poteomkin, A. M. Sergeev, A. A. Shaykin, and I. V. Yakovlev, “Compact 0.56 petawatt laser system based on optical parametric chirped pulse amplification in KD*P crystals,” *Laser Phys. Lett.* **4**, 421 (2007).
- ¹¹T. Baeva, S. Gordienko, and A. Pukhov, “Theory of high-order harmonic generation in relativistic laser interaction with overdense plasma,” *Phys. Rev. E* **74**, 046404 (2006).

¹²C. Rödel, D. an der Brügge, J. Bierbach, M. Yeung, T. Hahn, B. Dromey, S. Herzer, S. Fuchs, A. Pour, E. Eckner, M. Behmke, M. Cerchez, O. Jäckel, D. Hemmers, T. Toncian, M. Kaluza, A. Belyanin, G. Pretzler, O. Willi, A. Pukhov, M. Zepf, and G. Paulus, “Harmonic generation from relativistic plasma surfaces in ultrasteep plasma density gradients,” *Phys. Rev. Lett.* **109**, 125002 (2012).

¹³F. Dollar, P. Cummings, V. Chvykov, L. Willingale, M. V. and V. Yanovsky, C. Zulick, A. Maksimchuk, A. Thomas, and K. Krushelnick, “Scaling high-order harmonic generation from laser-solid interactions to ultrahigh intensity,” *Phys. Rev. Lett.* **110**, 175002 (2013).

¹⁴F. Wagner, C. Brabetz, O. Deppert, M. Roth, T. Stöhlker, A. Tauschwitz, A. Tebartz, B. Zielbauer, and V. Bagnoud, “Accelerating ions with high-energy short laser pulses from submicrometer thick targets,” *High Power Laser Sci. Eng.* **4**, e45 (2016).

¹⁵A. Soloviev, K. Burdonov, S. Chen, A. Ereemeev, A. Korzhimanov, G. Pokrovskiy, T. Pikuz, G. Revet, A. Sladkov, V. Ginzburg, E. Khazanov, A. Kuzmin, R. Osmanov, I. Shaikin, A. Shaykin, I. Yakovlev, S. Pikuz, M. Starodubtsev, and J. Fuchs, “Experimental evidence for short-pulse laser heating of solid-density target to high bulk temperatures,” *Sci. Rep.* **7**, 12144 (2017).